Photoluminescence of ultrasmall Ge quantum dots grown by molecular-beam epitaxy at low temperatures

M. W. Dashiell,[a] U. Denker, C. Müller, G. Costantini, C. Manzano, K. Kern, and O. G. Schmidt
Max-Planck-Institut für Festkörperforschung, Heisenbergstraße 1, 70569 Stuttgart, Germany

(Received 19 June 2001; accepted for publication 7 November 2001)

Low-temperature epitaxial growth of Si–Ge heterostructures opens possibilities for synthesizing very small and abrupt low-dimensional structures due to the low adatom surface mobilities. We present photoluminescence from Ge quantum structures grown by molecular-beam epitaxy at low temperatures which reveals a transition from two-dimensional to three-dimensional growth. Phononless radiative recombination is observed from ⟨105⟩ faceted Ge quantum dots with height of approximately 0.9 nm and lateral width of 9 nm. Postgrowth annealing reveals a systematic blueshift of the Ge quantum dot's luminescence and a reduction in nonradiative recombination channels. With increasing annealing temperatures Si–Ge intermixing smears out the three-dimensional carrier localization around the dot. © *2002 American Institute of Physics.* [DOI: 10.1063/1.1430508]

The 4% lattice mismatch between Ge and Si drives the self-assembly of Ge islands[1] via the Stranski–Krastanov (SK) growth mode which, in addition to other mechanisms such as C-induced Ge quantum dot (QD) formation,[2–4] offers a pathway to enhancing the optical performance of Si-based heterostructures. Prior investigations of the electronic structure of SK Ge islands have concentrated on the optical properties of Ge islands grown at temperatures greater than 500 °C.[5,6] Under these conditions, the islands undergo Si–Ge intermixing, resulting in alloyed islands with typical lateral dimensions above 50 nm. Approaches to reduce intermixing and to customize the size of self-assembled QDs include: (i) minimizing surface diffusion by lowering the growth temperature[7] and reducing the Si overgrowth temperature,[8] and (ii) the predeposition of impurity atoms such as B (Ref. 9) or C.[2–4] While the latter approaches (ii) have produced high densities of small QDs, the impurities influence the electronic properties of the dots. There are sparse data on the optical properties of very-small and pure Ge islands synthesized at low ($\leqslant$ 500 °C) temperatures.[10–12] At these growth temperatures, low-adatom mobilities often impede high-quality epitaxy and also may kinetically limit island formation.[7]

In this letter, we present photoluminescence (PL) investigations of single-layer Ge structures formed at low growth temperatures (T_g) and Ge growth rate (r_g) of 0.125 monolayer (ML) per minute. The low Ge growth rate was chosen to overcome kinetic barriers to island nucleation that are anticipated at reduced T_g and was based upon the surface-adatom diffusion length $L=(D_s\tau)^{1/2}$ relevant for island formation, where D_s is the surface diffusion coefficient of adatoms and τ is the adatom residence time ($\tau\sim 1/r_g$). Assuming that the limited surface diffusion is the primary factor controlling the morphological transition from two-dimensional (2D) to three-dimensional (3D) island growth, we chose r_g so the corresponding increase in τ will roughly compensate for the decrease in D_s at 360 °C, i.e., our calculated value of L was comparable to values we calculated for conventional Ge island growth conditions. The values for D_s were taken from experimental values determined for Ge adatoms on 1 ML of Ge grown on Si(001).[13]

Samples were grown by solid-source molecular-beam epitaxy[12] (MBE) on p^--Si substrates that were chemically cleaned, loaded into the growth chamber, then deoxidized at 900 °C and 60 nm Si buffers were grown at 500 °C. Prior to Ge deposition, the substrate temperature was ramped during Si growth to T_g. The Ge monolayers were then deposited and subsequently capped at T_g with 100 nm Si for PL studies. The Ge layer sequence was repeated at the surface for morphological analysis by means of *ex situ* atomic-force microscopy (AFM) and *in situ* scanning tunneling microscopy (STM). The latter is a home-made ultra-high-vacuum (UHV) apparatus, directly attachable to the MBE, and is analogous to the STM reported in Ref. 14.

Figures 1(a)–1(c) display images of Ge island samples grown between 500 and 360 °C. The 8 K PL spectra from as-grown samples (5.6 ML Ge) are shown in Fig. 1(d). Ge hut clusters,[1] elongated in ⟨001⟩ and with 1.2 nm height and base width of between 20 and 30 nm are observed for $T_g = 500$ °C [Fig. 1(a)]. These huts emit a PL signal centered around 0.8 eV,[11] which was recently shown to originate from spatially indirect, phononless carrier recombination between holes confined in the Ge huts and electrons confined in surrounding tensile-strained Si.[12] Lowering T_g to 450 °C also results in slightly smaller hut clusters (height ~1.0 nm) than those grown at 500 °C. A PL intensity reduction of greater than 50% is observed from these hut clusters, as well as a high-energy shoulder. Decreased PL intensity is attributed to nonradiative recombination channels related to point defects that form at lower T_g. The high-energy shoulder was also observed in the sample grown at 500 °C for Ge deposition slightly above the transition thickness for 2D to 3D growth, suggesting that the shoulder originates from the flat Ge wetting layer (WL). Upon further reduction of T_g to 360 °C, very small surface structures appear that no longer appear to be elongated in any discernable crystallographic orientation

[a]Electronic mail: dashiell@servix.mpi-stuttgart.mpg.de

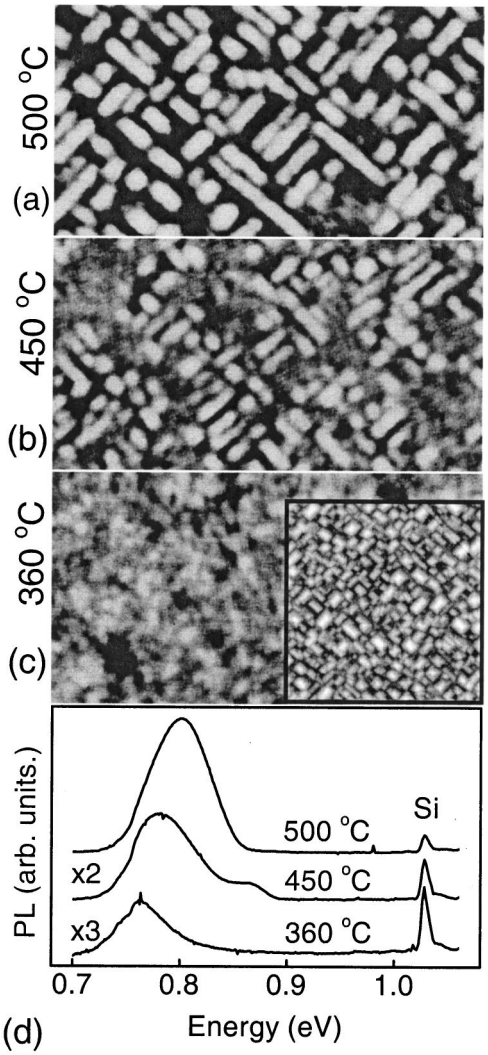

FIG. 1. 500 nm×250 nm AFM images of 5.6 ML nominal Ge thickness deposited at (a) 500 °C, (b) 450 °C, and (c) 360 °C. The inset of (c) is on the same scale (230 nm×230 nm) and displays an *in situ* STM topograph (filled states, 0.2 nA, −3 V) of a 5.6-ML-thick Ge layer grown at 360 °C. (d) 8 K PL spectra of the Ge QDs grown at the three T_g values indicated. The Si phonon-assisted PL reference peak ($TO+O^{\Gamma}$) is observed at energy 1.035 eV.

in the AFM scan of Fig. 1(c). The inset of Fig. 1(c) shows an *in situ* STM image of the sample grown under equivalent conditions, which reveal a high density of very small Ge hut clusters; vertical and lateral sizes of the huts are 0.8 ± 0.2 and 9 ± 1 nm, respectively, with facet angles of $11°\pm1°$ corresponding to the {105} planes. PL emission at 765 meV, having a 44 meV full width at half maximum (FWHM) is detected from the single Ge dot layer grown at $T_g=360$ °C, however the intensity has decreased to nearly 10% of the intensity of the hut clusters grown at 500 °C. A redshift of the PL emission compared to the huts formed at 500 °C can be explained by reduced Si–Ge intermixing during growth and Si capping. We note that a similar PL spectrum was observed in sixfold stacked Ge layers grown at 250 °C,[10] however, a systematic study was not performed to exclude the possibility that the PL may originate from defect bands sometimes found near similar energies in dislocated or damaged Si/Ge/Si structures.[15,16]

PL emission energies from Si/Ge/Si quantum structures vary systematically with total deposited Ge thickness due to

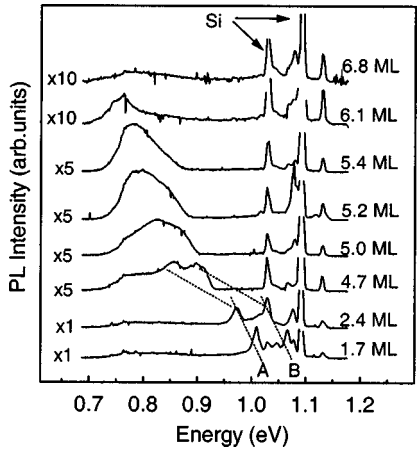

FIG. 2. 8 K PL spectra from as-grown Ge layers ($T_g=360$ °C) having various Ge coverage. Evolution from quantum-well-like to quantum-dot-like emission can be observed above 4.7 ML.

quantum-confinement effects.[5,11] Figure 2 displays the 8 K PL spectra from our single Ge layers ($T_g=360$ °C) with total nominal thicknesses ranging from 1.7 to 6.8 ML. For 2.4 ML and below we observe two peaks, labeled A and B separated by 55 meV, that redshift (see dotted guide lines) with increasing Ge deposition. Peaks A and B are attributed to recombination within flat Ge WLs, where A is the transverse optical (TO) phonon replica of the no-phonon (NP) peak labeled B.[5] Upon further Ge deposition, peaks A and B evolve into a broad peak that continues to redshift with increasing Ge deposition corresponding to the transition from 2D to 3D Ge layer growth observed with AFM. Our thickness dependence of Ge-related PL exhibits behavior similar to that observed for SK Ge islands grown at temperatures from 500 to 700 °C, where the redshifts are due to the influence of WL thickness and island size on quantum-confined energy levels.[5,6,11] We note that above 6 ML, the Ge-related PL intensity rapidly quenches, suggesting that the structural integrity of the layer degrades above a critical thickness.

Figure 3(a) displays the 8 K PL spectra from Ge QDs ($T_{\text{growth}}=360$ °C) with 5.4 ± 0.2 ML nominal thickness after

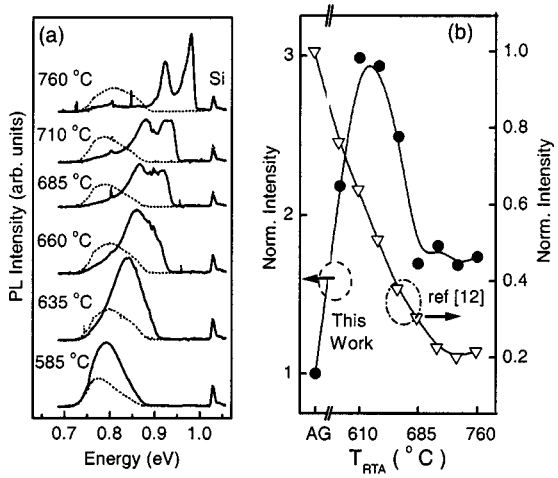

FIG. 3. (a) 8 K PL spectra from single layers of Ge QDs after selected 60 s RTA anneals (solid lines). The preannealing spectra are included as dotted lines. (b) The total integrated Ge-related PL intensity, normalized to its preannealing intensity, as a function of T_{RTA} for the ultrasmall Ge QDs ($T_g=360$ °C) and the Ge hut clusters ($T_g=500$ °C) from Ref. 12.

postgrowth rapid thermal anneals (RTAs) in forming gas at temperatures T_{RTA}. Included are the reference spectra of the samples prior to annealing (dotted lines). Increase of the Ge-related PL intensity, relative to the preannealing intensity, is evident for all T_{RTA} values, as is a systematic blueshift of peak PL energies. Increased PL intensity after postgrowth annealing is attributed to reduction of point defect densities,[17,18] which in this case probably result from low T_g. For T_{RTA} up to 660 °C, the Ge QD PL peak blueshifts, yet retains its single broad PL peak. Such a blueshift is typically observed in $Si_{1-x}Ge_x$ quantum structures and Ge dots due to Si–Ge intermixing.[12,18,19] Above $T_{RTA}=660$ °C, a gradual transition to two well-resolved emission bands, separated in energy by 55 meV, reflects the transition from quantum-dot-like to a quantum-well-like PL spectra; this occurs as the Ge dot's 3D confinement potential becomes smeared out.[12,18] The systematic blueshift and transition from dot-like to well-like PL are further proof that the PL does not originate from misfit dislocations nucleated during the growth. We explain the very limited thermal stability in these Ge QDs by enhanced Si–Ge intermixing observed during annealing of modulated Si/Ge heterostructures. Strain and compositional gradients resulted in enhanced intermixing across the interfaces of $(Si_mGe_n)_p$ superlattices (SLs) at annealing temperatures as low as 550 °C; it was suggested that the intermixing was governed by the vacancy-assisted diffusion of Si into Ge.[20] This process accounts for our observed blueshift with increasing T_{RTA} (i.e., as the average Si content in the small QD increases). Carrier localization at the Si–Ge interface plays a strong role on the phononless (i.e., dot-like) PL from Ge islands embedded within Si,[12] thus intermixing across the abrupt interface can explain the rapid quenching of the dot-like PL for $T_{RTA}>635$ °C. After a critical degree of intermixing across the dot interface, the PL reflects that the confining potential resembles an inhomogeneously thick quantum well (deduced by the transition to phonon-assisted PL and the nearly 50% increase in QW PL linewidths compared to our 2D Si/Ge/Si samples annealed under the same conditions).

Figure 3(b) displays, for various T_{RTA}, the integrated PL intensity from the ultrasmall Ge QDs normalized to their as-grown intensity (this work, solid markers) and from the hut clusters grown at $T_g=500$ °C within the same MBE chamber[12] (hollow markers). The phononless PL originating from the Ge hut clusters ($T_g=500$ °C), monotonically decreases upon annealing for T_{RTA} up to 700 °C due to atomic-scale Si–Ge intermixing and the resultant decrease of the interface localization potential.[12] In contrast, for $T_{RTA}<635$ °C we observed a sharp increase in integrated intensity from the Ge QDs presented in this letter; only after an optimal value of T_{RTA} does the PL intensity begin to decrease. The nonmonotonic intensity dependence of the Ge QDs grown during this work ($T_g=360$ °C) can be explained by two competing mechanisms. First, healing out of point defects formed at low T_g initially increase the PL intensity with T_{RTA}. The Ge hut clusters of Ref. 12 were grown at 500 °C, so the initial density of nonradiative channels should be much less compared to samples grown at 360 °C. As T_{RTA} is increased from 610 to 685 °C, however, the PL intensity from Ge QDs grown at 360 °C decreases at a rate similar to those of Ref. 12. This suggests that the rate of defect healing becomes insignificant compared to the effect of smearing out the 3D localization potentials. For both structures, the PL intensity saturates for $T_{RTA}>700$ °C, i.e., at the transition from dot-like to well-like PL. The PL evolution of the ultrasmall Ge QDs ($T_g=360$ °C) suggests that the PL originates from spatially indirect recombination of confined carriers, as proposed in Ref. 12.

In summary, we have investigated the PL properties of ultrasmall Ge QDs grown at low temperatures. Redshift with increasing Ge deposition and diffusion-driven blueshifts of the quantum-dot PL band indicate that carriers are localized within 3D confined energy states in a type-II band alignment, as proposed in Ref. 12. The phononless PL intensity is degraded because of the low-temperature growth, however, annealing studies indicate that PL intensity is partially restored after postgrowth RTA annealing. RTA conditions must be carefully optimized because of the competing influences of point defect reduction and Si–Ge intermixing on the phononless QD PL intensity.

One of the authors (M.W.D.) acknowledges financial support from a Max-Planck-Gesellschaft Stipendium.

[1] Y. W. Mo, D. E. Savage, B. S. Schwartzentruber, and M. G. Lagally, Phys. Rev. Lett. **65**, 1020 (1990).
[2] O. G. Schmidt, C. Lange, K. Eberl, O. Kienzle, and F. Ernst, Appl. Phys. Lett. **71**, 2340 (1997).
[3] O. G. Schmidt, K. Eberl, and J. Auerswald, J. Lumin. **80**, 491 (1998).
[4] O. G. Schmidt, C. Lange, K. Eberl, O. Kienzle, and F. Ernst, Thin Solid Films **321**, 70 (1998).
[5] H. Sunamura, S. Fukatsu, N. Usami, and Y. Shiraki, Appl. Phys. Lett. **63**, 1651 (1993).
[6] P. Schittenhelm, M. Gail, J. Brunner, J. F. Nützel, and G. Absteiter, Appl. Phys. Lett. **67**, 1292 (1995).
[7] B. J. Spencer, P. W. Vorhees, and S. H. Davies, J. Appl. Phys. **73**, 4955 (1993).
[8] O. G. Schmidt, U. Denker, K. Eberl, O. Kienzle, and F. Ernst, Appl. Phys. Lett. **77**, 2509 (2000).
[9] H. Takamiya, M. Miura, N. Usami, T. Hattori, and Y. Shiraki, Thin Solid Films **369**, 84 (2000).
[10] V. A. Markov, H. H. Cheng, C.-t. Chia, A. I. Nikiforov, V. A. Cherepanov, O. P. Pchelyakov, K. S. Zhuraylev, A. B. Talochkin, E. McGlynn, and M. O. Henry, Thin Solid Films **369**, 79 (2000).
[11] O. G. Schmidt, C. Lange, and K. Eberl, Appl. Phys. Lett. **75**, 1905 (1999).
[12] M. W. Dashiell, U. Denker, and O. G. Schmidt, Appl. Phys. Lett. **79**, 2261 (2001).
[13] M. G. Lagally, Jpn. J. Appl. Phys., Part 1 **32**, 1493 (1993).
[14] O. Leifeld, B. Mueller, D. A. Gruetzmacher, and K. Kern, Appl. Phys. A: Mater. Sci. Process. **66**, S993 (1998).
[15] J. C. Sturm, A. St. Amour, Y. Lacroix, and M. L. W. Thewalt, Appl. Phys. Lett. **64**, 2291 (1994).
[16] R. Sauer, J. Weber, J. Soltz, E. R. Weber, K. H. Küsters, and H. Alexander, Appl. Phys. A: Solids Surf. **36**, 1 (1985).
[17] S. Fukatsu, N. Usami, and Y. Shiraki, J. Vac. Sci. Technol. B **11**, 895 (1993).
[18] S. Schieker, O. G. Schmidt, K. Eberl, N. Y. Jin-Phillipp, and F. Phillipp, Appl. Phys. Lett. **72**, 3344 (1998).
[19] H. Sunamura, S. Fukatsu, N. Usami, and Y. Shiraki, Appl. Phys. Lett. **63**, 1651 (1993).
[20] J.-M. Baribeau, R. Pascual, and S. Saimoto, Appl. Phys. Lett. **57**, 1502 (1990).